

# Software Resolver-to-Digital Converter for Compensation of Amplitude Imbalances using D-Q Transformation

Youn-Hyun Kim<sup>\*</sup> and Sol Kim<sup>†</sup>

**Abstract** – Resolvers are transducers that are used to sense the angular position of rotational machines. The analog resolver is necessary to use resolver to digital converter. Among the RDC software method, angle tracking observer (ATO) is the most popular method. In an actual resolver-based position sensing system, amplitude imbalance dominantly distorts the estimate position information of ATO. Minority papers have reported position error compensation of resolver's output signal with amplitude imbalance. This paper proposes new ATO algorithm in order to compensate position errors caused by the amplitude imbalance. There is no need premeasured off line data. This is easy, simple, cost-effective, and able to work on line compensation. To verify feasibility of the proposed algorithm, simulation and experiments are carried out.

**Keywords:** Resolver-to-Digital converter (RDC), Synchronous demodulation, Angle Tracking Observer (ATO), Amplitude unbalance

## 1. Introduction

Modern servo-drive systems often require the measurement of the motor-shaft angle or speed [1]. Rotor position information is essential in vector control for high performance motor drive [5].

Resolvers are transducers that are used to sense the angular position of rotational machines. They resemble small motors and have electro-magnetically coupled rotor and stator windings [12].

Resolvers are low cost and simple absolute angle transducer, providing two output signals that always allow the detection of the absolute angular position information. In addition, resolvers suppress common-mode noise and especially useful in noisy environments.

Compared with other kinds of position sensors, resolvers have some advantages. They are operating in harsh environmental condition and good endurance in high rotational speeds and accelerations. They have high reliability, accuracy, and mechanical durability in wide temperature ranges. They are possible to transmit output data signal across a long distance. Such advantages make resolver particularly suitable to severe industrial environments including automotive, space, radar, and robot applications [1-3].

The resolver output signals are analog signals, so the resolver signals should be converted to digital data to utilize in modern control system [5]. This conversion is made by means of so-called Resolver-to-Digital Converter

(RDC). These are integrated circuit which can be easily mounted on the motor control board [1]. Currently, most of these decoders are based on feedback-control loops aiming to match an estimated angle to the real angle [9].

The main demerit of the RDC is high cost, which is about the same price as that of the resolver [4]. For this reason, many efforts have been focused on finding low-cost R/D converter topologies [1].

Recently, many papers have been reported to propose simple and cost-effective methods in order to avoid the use of RDCs [1, 4, 5, 7-11].

Typically, two approaches are well known for RDC. First method is a software access method and second is a hardware access method. Tangential method, ATO (Angle Tracking Observer), etc. belong to the software access method. Among the software method, ATO is the most popular method.

The most of ATO papers suggest their own algorithm under the assumption that ideal resolver signals are supplied to the converter. In real industrial field, no resolver generates ideal signals and thus the accuracy specifications of an R/D converter can never be met in practice. In an actual resolver-based position sensing system, amplitude imbalance, quadrature error, inductive harmonics, reference phase shift, excitation signal distortion, and disturbance signals all exist due to the finite precision with which a resolver can be mechanically constructed and electrically excited [14]. Due to these nonideal characteristics of the resolver signals, the estimate position information of ATO can be considerably distorted. In particular, the amplitude imbalance is dominant component [3].

Minority papers have reported position error compensation of resolver's output signal with amplitude imbalance [3, 6,

<sup>†</sup> Corresponding author: Dept. of Electrical Engineering, Yuhan College, Korea (slamsol@yuhan.ac.kr)

<sup>\*</sup> Dept. of Electrical Engineering, Hanbat University, Korea (yhyunk@hanbat.ac.kr)

Received: February 7, 2013; Accepted: April 18, 2013

15, 16].

H. S. Mok et al introduced to reduce the torque ripple caused by the amplitude imbalance [15]. J. Bergas et al did not explain concretely how the error by amplitude imbalance was compensated [6]. S. H. Hwang et al estimated error compensating angle from motor control current  $I_{dse}$  after analyzing position error caused by amplitude imbalance with synchronous  $d, q$  current using park's transformation. However, this method seemed to take many computation time and the chances of a truncation error in occurring in computation would be high [3].

The method proposed in [16] was only presented to integrate the ideal rotor position to get the magnitude of position error according to the distorted rotor position due to the amplitude imbalance. In addition, magnitude of position error is necessary to measure at pre-experimentation.

Therefore, this paper proposes new ATO algorithm in order to compensate position errors caused by the amplitude imbalance. This is easy, simple and software based cost-effective. Especially, there is no need premeasured off line data. It is able to work on line compensation. To verify feasibility of the proposed algorithm, simulation and experiments are carried out.

## 2. RDC and imbalancing problem

### 2.1 Software access method of RDC

Resolvers are used most often as angle-measurement transducers, in which 'analog' outputs are converted to a 'digital' format using R/D converter. [1]

The schematic electrical structure of a resolver is shown in Fig. 1.

The primary winding is supplied with a sinusoidal excitation voltage of 1-10kHz.

$$V_s = A' \sin(\omega t) \quad (1)$$

These results in the separate output signals on two secondary windings generated. The output voltages include sine signal and cosine signal. If the angular frequency of the primary excitation is very high with respect to the

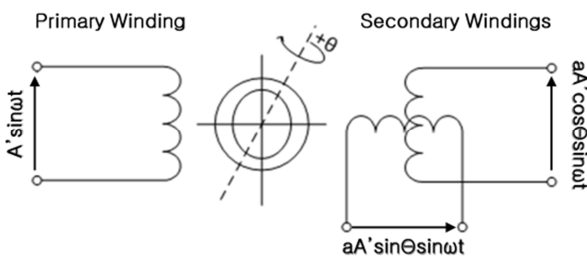


Fig. 1. The schematic electrical structure of a resolver

speed, the output voltages from the two secondary windings are amplitude modulated and can be expressed as follows;

$$V_s = aA' \sin \theta \sin \omega t \quad (2)$$

$$V_c = aA' \cos \theta \sin \omega t \quad (3)$$

where  $\theta$  is the angular position of rotor and  $a$  is a constant representing the transformation ratio between stator and rotor winding.

The output voltages require demodulation process and the obtained signals after demodulation are denoted as below.

$$V_{sm} = A' \sin \theta \quad (4)$$

$$V_{cm} = A' \cos \theta \quad (5)$$

This paper estimates position using the synchronous demodulation method [10] that detects and digitalizes peak values of  $\sin$  and  $\cos$  signal of resolver.

In general, the period of the current control of motor controller is 100μsec. The current controller is necessary to rotor position. Therefore, this paper squares magnetizing frequency as 10kHz with current controlling frequency of motor controller. Fig. 2 shows the demodulation process. The demodulated  $\sin$  and  $\cos$  signals are decided by sampling peak values of  $\sin$  and  $\cos$  in a period.

After demodulation, ATO algorithm extracts both position and speed from the demodulated  $\sin$  signal and  $\cos$  signal. This observer contains of a closed loop which compares permanently the real position  $\theta$  to the estimated position  $\phi$  [10].

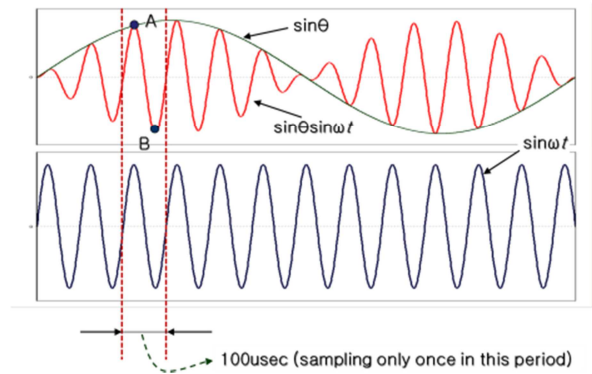


Fig. 2. Sampling of output signal

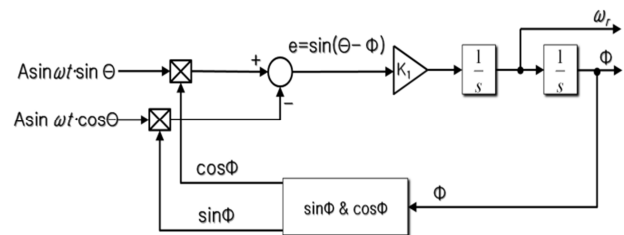


Fig. 3. Block diagram of the simplified ATO

Fig. 3 shows the common systemic diagram of the existing ATO closed-loop system. The observation error between the real position  $\theta$  and the estimated position  $\phi$  can be expressed as

$$e = \sin\theta \cdot \cos\phi - \cos\theta \cdot \sin\phi = \sin(\theta - \phi) \quad (6).$$

Finally, this error is driven to zero by ATO closed-loop with  $\phi$  being the control variable. When this is done, the estimated position  $\phi$  results in zero position error.

## 2.2 Imbalancing problem

RDC theories above chapter 2.1 assume that the resolver has no systematic errors caused by amplitude imbalances.

Amplitude imbalance between the two resolver signals is the most prevalent nonideal resolver signal characteristics. It may be generated due to the unbalanced excitation and unequal inductance of the resolver signals and due to the nonideal characteristics of analog devices.

If unbalanced output signal shows up on the sampling signal of resolver as Fig. 4, the resolver outputs with the amplitude imbalance can be expressed as

$$V_s = A \sin\theta \sin\omega t \quad (7)$$

$$V_c = A(1 + \alpha) \cos\theta \sin\omega t \quad (8)$$

where  $\alpha$  represents the amount of imbalance between the two signals.

Demodulating resolver outputs with the amplitude imbalance, the error voltage in Eq. (6) can be rewritten as

$$E = V_1 \{ \sin(\theta - \phi) - \alpha \cos\theta \sin\phi \} \quad (9).$$

Driving this error to zero, as commanded by the ATO tracking loop, does not lead to the desired solution  $\theta = \phi$  and the error of position estimation is same as Eq. (10).

$$\theta_{err} = \frac{\alpha}{2} \sin(2\theta) \quad (10)$$

Therefore, the error is sinusoidal with respect to position and has approximately twice the rotor position and has peak amplitude that is one half the amplitude of the amount

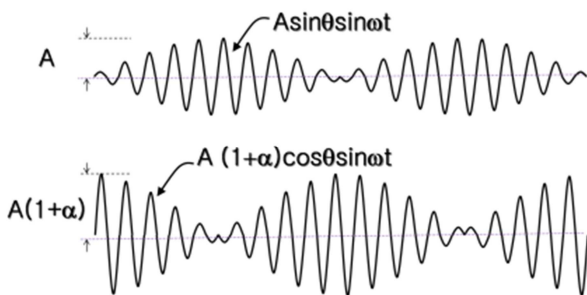


Fig. 4. Unbalanced sinusoidal signals of resolver's output

of imbalance [3, 14].

## 3. The proposed RDC Proposed Method

### 3.1 Explanation on the $d, q$ coordinates conversion

The modulated resolver output signal can be expressed as vector  $\vec{V}$  indicated in the following Eq. (11) that has amplitude  $A$  and position  $\theta$ .

$$\vec{V} = A \cos\theta + j A \sin\theta \quad (11)$$

This vector  $\vec{V}$  can be expressed as  $d, q$  axis in Fig. 5, revolving coordinate axis by using Park transformation. For arbitrary estimated position  $\phi$ , the  $d, q$  axis factor  $D_r$  and  $Q_r$  of vector  $\vec{V}$  for resolver output signal will be as expressed in Eq. (12).

$$\begin{bmatrix} D_r \\ Q_r \end{bmatrix} = \begin{bmatrix} \cos\phi & \sin\phi \\ -\sin\phi & \cos\phi \end{bmatrix} \begin{bmatrix} A \cos\theta \\ A \sin\theta \end{bmatrix} \quad (12)$$

The above Eq. (12) is arranged as the following Eqs. (13) and (14).

$$D_r = A(\sin\theta \sin\phi + \cos\theta \cos\phi) = A \cos(\theta - \phi) \quad (13)$$

$$Q_r = A(\sin\theta \cos\phi - \cos\theta \sin\phi) = A \sin(\theta - \phi) \quad (14)$$

If an arbitrary estimated position  $\phi$  coincides with actual position  $\theta$ , namely if  $\theta - \phi = 0$ ,  $\vec{V}$  coincides with  $d$  axis as shown in Fig. 5 and thus only  $d$  axis factor,  $D_r$  value exists and  $q$  axis factor  $Q_r$  becomes zero. This is also calculated by Eqs. (13) and (14) and  $D_r$  value becomes maximum value  $A$  and  $Q_r$  becomes zero. The conventional ATO uses Eq. (14) to make  $Q_r$  converge to zero so that the estimated position  $\phi$  may correspond with actual position  $\theta$ . The tracking method to set the estimated position  $\phi$  to actual position  $\theta$  so as to make  $D_r$  of Eq. (13) converge to maximum value  $A$  can make convergence if the amplitude ratio of  $\sin$  and  $\cos$  output is same, but  $\cos(\theta - \phi)$  for  $\theta$  is even function and the change of  $\cos\theta$  is small near

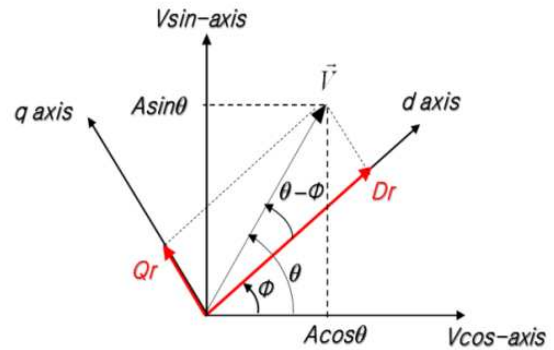


Fig. 5. Revolving coordinate axis  $d, q$  axis for resolver signals.

$(\theta - \phi) = 0$ . Thus, convergence time and precision are problematic. As a result, convergence time and precision are lower than that of  $Q_r = 0$  convergence. Further, if amplitude ratio is different,  $D_r$  is converged at two points without guaranteeing stable convergence. As there is diverging area, additional convergence conditions should be added. Thus, the conventional general ATO uses the method of  $Q_r = 0$ . This paper does not directly utilize method of  $D_r = \text{Max}$  to estimate position but propose algorithm to compensate the position error by amplitude imbalance of resolver output signals, based on the variation in position of  $D_r$ .

### 3.2 Proposed RDC theory

If resolver generates the output signals with different amplitude, namely, sine signal  $A \sin \theta \sin \omega t$  and cosine signal  $A(1 + \alpha) \cos \theta \sin \omega$ , the  $d$  axis factor  $D_r$  in Fig. 5 is acquired by multiplying and adding  $\cos \phi$  and  $\sin \phi$  of the estimated position to the demodulated amplitude imbalance of output signals. Then, unlike the above Eq. (13) where the amplitude of  $\sin$  signal and  $\cos$  signal is balanced, the following Eq. (15) is established.

$$D_r = A(\sin \theta \sin \phi + (1 + \alpha) \cos \theta \cos \phi) / A[\cos(\theta - \phi) + \alpha \cos \theta \cos \phi] \quad (15)$$

Further, if acquiring  $q$  axis factor  $Q_r$  in Fig. 5 by multiplying and subtracting  $\cos \phi$  and  $\sin \phi$  with the estimated position to the demodulated  $\sin$  &  $\cos$  signals in different amplitude, the following Eq. (16) is established unlike the above Eq. (14).

$$Q_r = A(\sin \theta \cos \phi - (1 + \alpha) \cos \theta \sin \phi) / A[\sin(\theta - \phi) - \alpha \cos \theta \sin \phi] \quad (16)$$

When the first term;  $A \cos(\theta - \phi)$  of  $D_r$  in the above Eq. (15) follows the conventional tracking position, it would be a constant as  $A$  since  $\theta = \phi$ . Although there is an error in position due to unbalanced amplitude of outputs, the value changes minutely because  $\theta$  is close to  $\phi$ . For instance, although the error;  $e = \theta - \phi$  is 10 degree, the change is about  $0.015 \times A$ . Thus, the most of change in  $D_r$  is affected by the second term;  $A \alpha \cos \theta \cos \phi$ . Therefore, if  $D_r$  is differentiated by the estimated position, it can be expressed by similar equation as shown in the following Eq. (17).

$$\frac{dD_r(\theta \cong \phi)}{d\phi} \cong \frac{d[A \alpha \cos \theta \cos \phi]}{d\phi} = -A \alpha \cos \theta \sin \phi \quad (17)$$

Thus, if subtracting the value of Eq. (17) from that of Eq. (16), the following Eq. (18) is established. Namely, the value can be that of Eq. (14) where the amplitude of resolver output signals is same as the  $A \alpha \cos \theta \sin \phi$

component of  $Q_r$  is eliminated, i.e., the component of position error by amplitude imbalance.

$$e = Q_r - \frac{dD_r(\theta \cong \phi)}{d\phi} \cong A \sin(\theta - \phi) \quad (18)$$

This paper presents ATO method so that  $Q_r - \frac{dD_r(\theta \cong \phi)}{d\phi}$  can be zero by using Eq. (18) which is not to make the  $Q_r$  of the conventional ATO converge towards zero.

Fig. 6 shows a block diagram of the proposed tracking observer covering amplitude imbalance. In Fig. 6, peak value of signal is sampled from 100  $\mu\text{sec}$  cycled position tracker. Then, the demodulated resolver's output signal  $A \sin \theta$ , which is converted into digital value by A/D conversion, is transformed into  $A \sin \theta \cos \phi$  by multiplying with  $\cos \phi$  which is made by cosine wave generator as controlled  $\phi$  to estimate position.

Further, the demodulated  $\cos$  signal  $A(1 + \alpha) \cos \theta$  is transformed into  $A(1 + \alpha) \cos \theta \sin \phi$  by multiplying  $\sin \phi$  which is made by sine wave generator as controlled  $\phi$  to track position.

$Q_r$  is obtained by subtracting  $A(1 + \alpha) \cos \theta \sin \phi$  from  $A \sin \theta \cos \phi$  as Eq. (16).

The subtraction from  $Q_r$  to the imbalance compensation is calculated in Eq. (18). By performing PI position tracking routine that regulates  $\phi$  to drive this difference to zero, the estimated position  $\phi$  is forced to equal the real position  $\theta$  resulting in zero position error.

The imbalance position error compensator of the dashed box of Fig. 6 estimates position with conventional ATO, which is to make converge  $Q_r$  to zero, tracks the estimated position  $\theta'$ . The period of excitation signal is identical to the motor current controller as 100  $\mu\text{sec}$ . The imbalance compensation value  $\frac{dD_r(\theta \cong \theta')}{d\theta'}$  is obtained from calculating last step value  $D_r[k - 1]$  and present step value  $D_r[k]$  and  $dD_r(\theta \cong \theta') = D_r[k] - D_r[k - 1]$  based on the estimated position  $\theta'$  substituting  $\omega_r \cdot dt$  for  $d\theta'$  where  $dt$  is 100  $\mu\text{sec}$ .

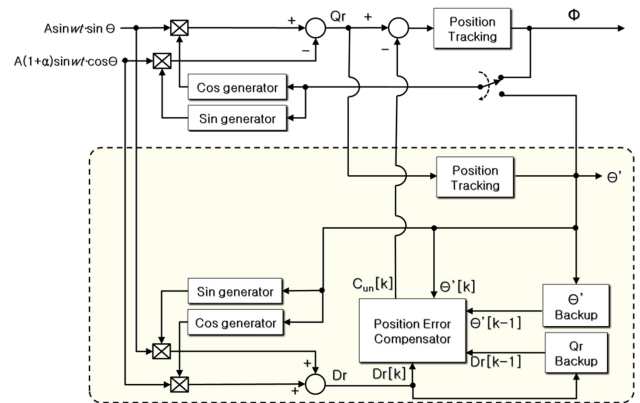


Fig. 6. The proposed tracking observer covering amplitude imbalance

$$C_{un} = \frac{dD_r(\theta=\theta')}{d\theta'} = \frac{dD_r(\theta=\theta')}{\omega_r \cdot dt} \quad (19)$$

Further,  $D_r[k]$  is calculated as Eq. (15) where  $\phi$  pertains to  $\theta'$  which is estimated for every 100  $\mu\text{sec}$  cycle.

The flowchart of the algorithm for the proposed tracking observer was presented in Fig. 7. If the position tracking routine begins, the initial values of position tracking,  $\phi[k]$  and  $\theta'[k]$  are set to estimating position  $\phi[k-1]$  of previous cycle. The imbalance compensation  $C_{un}$  in the dashed area is calculated by digitized sine and cosine signals of resolver output.

For calculation of imbalance compensation value, the method to converge to the conventional ATO method, which is  $Q_r = 0$ , is performed. To calculate  $C_{un} = \frac{dD_r(\theta=\theta')}{d\theta'}$  to compensate position error based on estimated position  $\theta'$  after convergence routine is finished,  $D_r[k]$  of Eq. (15) is calculated.  $dD_r(\theta = \phi) = D_r[k] - D_r[k-1]$  and new imbalance compensation value  $C_{un}$  is calculated by  $D_r$  and  $D_r[k-1]$  of previous cycle. Further, the result of present calculation  $D_r[k]$  is saved in  $D_r[k-1]$ .

After obtaining amplitude imbalance compensation

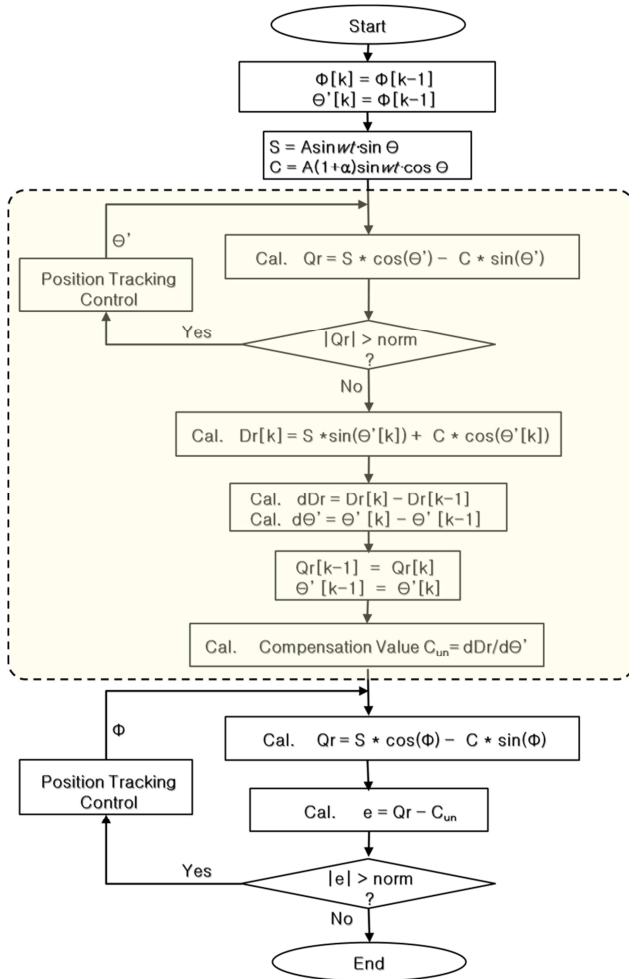


Fig. 7. The flowchart of the proposed tracking observer

value,  $e = Q_r - C_{un}$  is calculated in Eq. (18). Then,  $\phi$  is controlled iteratively until  $e$  value converges within error norm set to area near zero. When  $e$  converged within the error norm, we can regard the estimated position  $\Phi$  as the real position  $\theta$ .

If imbalance compensation value  $\frac{dD_r(\theta=\phi)}{d\phi}$  is perfect real position tracking in the proposed position estimation algorithm, only the imbalance term, the second term of Eq. (16) is calculated as the compensation value. However, the  $A \sin(\theta - \phi)$  term value remaining a bit in compensation value could be an error to imbalance compensation.

This paper shows the performance of the proposed position tracking observer when the resolver's output are not balanced. Analyzed simulation results are compared with experimental results.

## 4. Simulation and test result

### 4.1 Simulation results

Fig. 8 shows the simulation results of the conventional ATO when resolver generates sine and cosine output signals with amplitude imbalances. The simulation results contain position estimations when positions are estimated and the results of internal calculation values of imbalance position error compensation.

Fig. 8(a) is demodulated sin and cosine waveform of resolver.  $A$  and  $\alpha$  are setting up 1 and 0.5 respectively so that the amplitude of cosine output is 1.5 times larger than sine output.

When estimating position by the conventional ATO method, the real position  $\theta$  and the estimated position  $\phi$  are described in Figs. 8(b). In Fig. 8(b), the estimated position  $\phi$  as  $\sin(2\theta)$  cycle makes error and error  $(\theta - \phi)$  makes position error of approximately 14 degree to 1.5 times imbalance as shown in Fig. 8(c). Thus, the position error was generated as  $\frac{\alpha}{2} \sin(2\theta)$ .

Fig. 8(d) presents waveforms of  $Q_r$  and  $D_r$ .  $Q_r$  is nearly constant to zero since  $Q_r$  converges to zero by the conventional ATO. If  $D_r$  is not affected by amplitude imbalance, it would be constant as 1. However, it is changed to cycle of  $\cos 2\theta$  by the influence of the position error and amplitude imbalance as shown in the figure.

Fig. 8(e) shows the waveforms of the first term of  $Q_r$  value, namely,  $A \sin(\theta - \phi)$  and the second term  $-A \alpha \cos \theta \sin \phi$ .  $A \sin(\theta - \phi)$  means the position error and  $-A \alpha \cos \theta \sin \phi$  means the influence of amplitude imbalance. When estimating position by ATO,  $Q_r$  would be zero since the amplitude of the position error is same as that of influence of amplitude imbalance and their signs are the opposite.

Fig. 8(f) shows the waveforms of the first term of  $D_r$  value, namely,  $A \cos(\theta - \phi)$  and the second term  $A \alpha \cos \theta \cos \phi$ . In figure, the main reason of fluctuation in



$D_r$  is  $A\cos\theta\cos\phi$  caused by amplitude imbalance. If error  $(\theta - \phi)$  varies from 0 to 0.25 as radian value of 0 degree to 14 degree,  $A\cos(\theta - \phi)$  varies from 1 to 0.96891. Thus, the size of variation is minute as maximum 0.03109. On the contrary,  $A\cos\theta\cos\phi$  changes to size of 0.25 pertaining to  $\alpha/2$  to occupy most fluctuation of  $D_r$ .

Fig. 8(g) shows the waveforms of  $\frac{dD_r}{d\phi}$ ,  $A\cos\theta\sin\theta$  and their difference  $A\cos\theta\sin\theta - \frac{dD_r}{d\phi}$ .  $A\cos\theta\sin\theta$  is the factor where  $Q_r$  does not become perfect zero by the influence of amplitude imbalance although error  $(\theta - \phi)$  is zero and  $\frac{dD_r}{d\phi}$  is the differentiation of  $D_r$ . Figure shows that  $A\cos\theta\sin\theta$  is quite similar to the differentiation of  $D_r$ ,  $\frac{dD_r}{d\phi}$  and their difference is near zero. Thus, if getting  $\frac{dD_r}{d\phi}$  after the conventional ATO converges  $Q_r$  to zero,  $\frac{dD_r}{d\phi}$  becomes to amplitude imbalance term of  $Q_r$ . The simulation result explained that if excluding  $\frac{dD_r}{d\phi}$  from  $Q_r$ ,

only the value of  $A\sin(\theta - \phi)$  which purely excluded from the influence of amplitude imbalance can be extracted.

Fig. 9 shows the simulation results of the proposed ATO when resolver generates  $\sin$  and  $\cos$  output signal with amplitude imbalance. The simulation results contain position estimations when positions are estimated and the results of internal calculation values of imbalance position error compensation.

Like Figs. 9(a), this paper makes resolver outputs so that the amplitude of cosine output is 1.5 times larger than that of sin output as same as the simulation of conventional ATO. When estimating position by the proposed tracking observer algorithm, the real position  $\theta$  and the estimated position  $\phi$  is shown in Fig. 9(b) and the position error is also described in Fig. 9(c).

Fig. 9(b) and (c) showed that the estimated position  $\phi$  coincides with the real position  $\theta$  because the position error of  $\sin(2\theta)$  cycle by amplitude imbalance shown in the

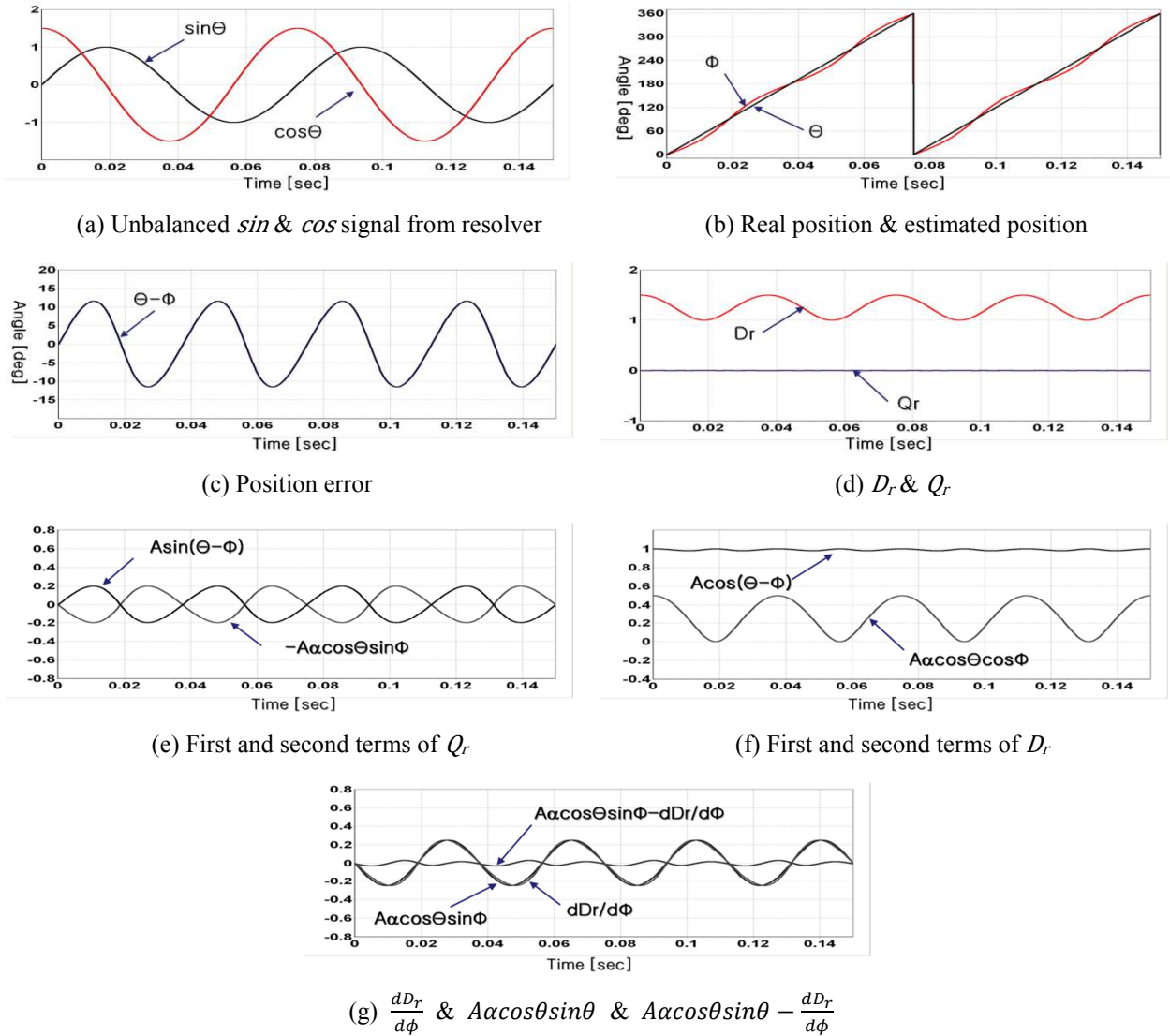


Fig. 8. Conventional ATO output signals when unbalanced resolver's output (simulation)

conventional method is compensated.

The waveforms of  $Q_r$  and  $D_r$  are shown in Fig. 9(d). It does not converge to make  $Q_r$  zero, but estimate to make  $e = Q_r - C_{un}$  converge to zero. As the estimated position  $\Phi$  nearly coincides with the real position  $\theta$ ,  $D_r$  is same as  $A\cos\theta\cos\phi$  that is the second term of Eq. (15) and  $Q_r$  is same as  $-A\cos\theta\sin\phi$  that is the second term of Eq. (16).

Fig. 9(e) shows the first term of  $Q_r$  value, namely,  $A\sin(\theta - \phi)$  and the second term  $-A\cos\theta\sin\phi$ . After all, the position error term  $A\sin(\theta - \phi)$  could be ignored since the difference between the estimated position  $\phi$  and the real position  $\theta$  is small. The most value of  $Q_r$  would be  $-A\cos\theta\sin\phi$  term caused by amplitude imbalance.

Fig. 9(f) shows the first term of  $D_r$  value  $A\cos(\theta - \phi)$  and the second term  $A\cos\theta\cos\phi$ . In figure, the main term of  $D_r$  is  $A\cos\theta\cos\phi$  cause by amplitude imbalance. As the difference between the estimated position  $\phi$  and the real position  $\theta$  is small,  $A\cos(\theta - \phi)$  will be a constant as almost 1.

Fig. 9(g) shows  $C_{un} = \frac{dD_r}{d\theta}$ ,  $A\cos\theta\sin\theta$  and their difference  $C_{un} - A\cos\theta\sin\theta$ . Figure shows that  $C_{un}$  and  $-A\cos\theta\sin\theta$  are more similar than that of the conventional ATO and the difference is closer to zero.

Therefore, we can verify that the proposed algorithm excellently tracks the real position eliminating the influence based on amplitude imbalance.

## 4.2 Experimental results

Fig. 10 shows the experimental results of the conventional ATO when resolver generates sine and cosine output signals with amplitude imbalances. The experimental results contain position estimations when positions are estimated and the results of internal calculation values of imbalance position error compensation.

Fig. 10(a) is the same condition as in the simulation; measurement was made when the demodulated resolver's

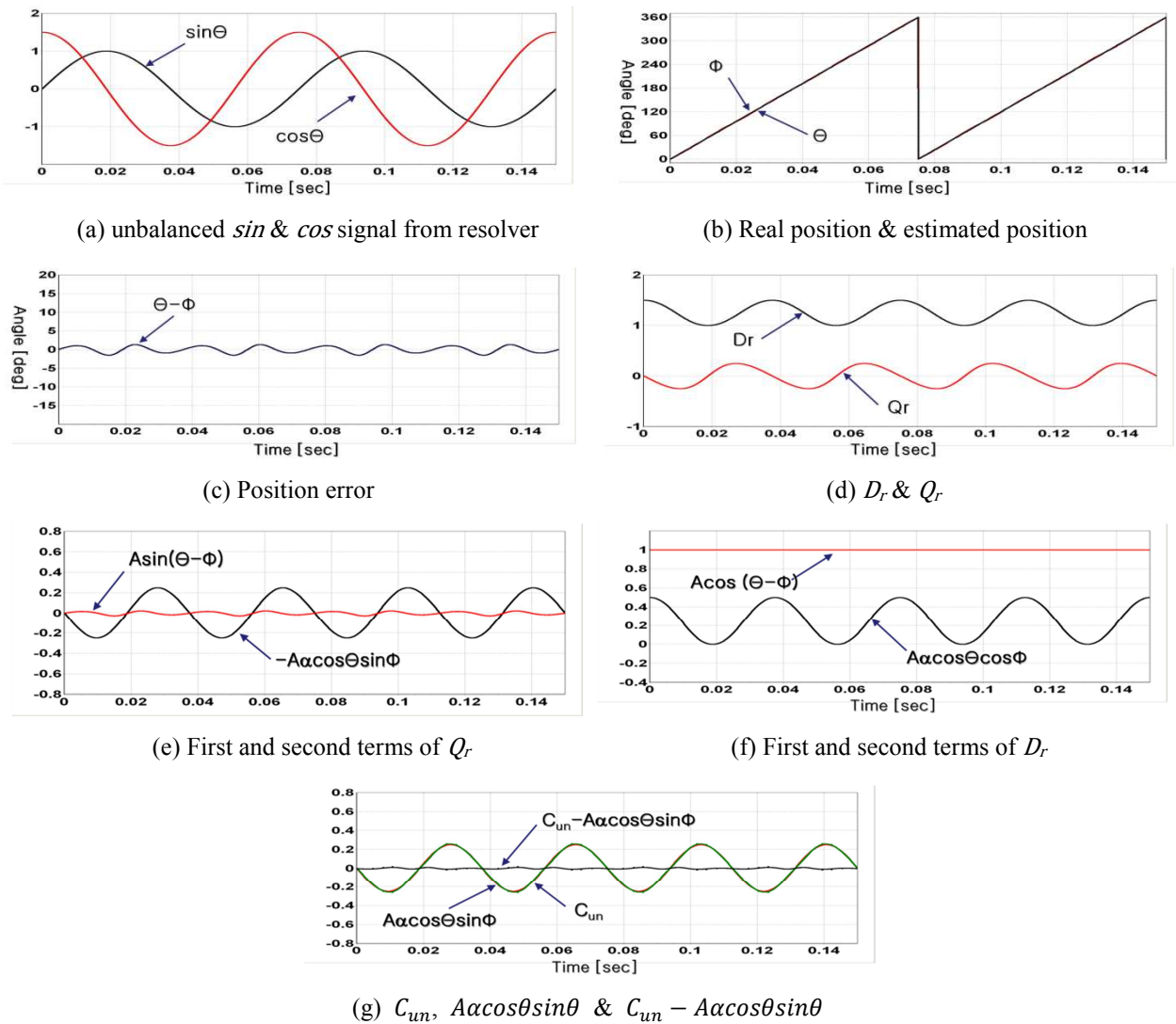


Fig. 9. Proposed ATO output signals when unbalanced resolver's output (simulation)

cosine output is 1.5 times larger than the sine output. Fig. 10(b) shows the real position  $\theta$  and the estimated position  $\phi$  when tested using the conventional ATO method. In the figure, it shows that the estimated position  $\phi$  has an error in every  $\sin 2\theta$  period as in the simulation.

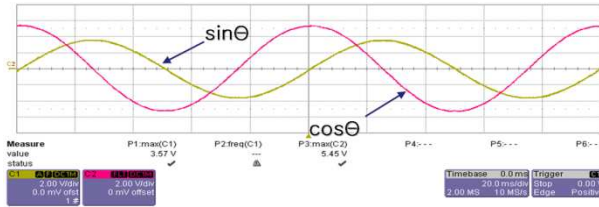
Fig. 10(d) is the waveforms of  $Q_r$  and  $D_r$ .  $Q_r$  regards as constant to 0 since  $Q_r$  converges to 0. Because of the influence by amplitude unbalance,  $D_r$  fluctuates in a period of  $\cos 2\theta$ . Fig. 10(e) shows the first term of  $O_r$ ,  $A \sin(\theta - \phi)$  and the second term  $-A \cos \theta \sin \phi$ . The result is similar with the simulation. Fig. 10(f) shows the waveforms of the first term of  $D_r$ ,  $A \cos(\theta - \phi)$  and the second term  $A \cos \theta \cos \phi$ . The main reason why  $D_r$  is fluctuating was also  $A \cos \theta \cos \phi$  influenced by amplitude imbalance as same as the simulation. Fig 10(g) shows the subtract of the differentiate of  $D_r$  which is  $\frac{dD_r}{d\phi}$  and the term influenced by amplitude unbalance which is  $A \cos \theta \sin \theta$  and their difference. As in the figure,  $\frac{dD_r}{d\phi}$  and  $A \cos \theta \sin \theta$  are

equal to that of the simulation. The experiment examined the simulation and the experimental results showed perfect match with the simulation.

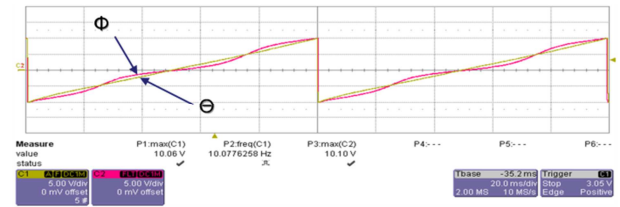
Fig. 11 also shows the experimental results of the proposed tracking algorithm. The estimation and internal calculation variables are plotted. The experimental condition is as the simulation.

As shown in fig 11(a), the resolver outputs were made the same result with the conventional ATO in experiment. When estimating the position by the proposed algorithm, the waveforms of real position  $\theta$  and the estimated position  $\phi$  are shown in fig 11(b). The position error is described in fig 11(c). With the periodic of  $\sin(2\theta)$ , position error occurred in the conventional method due to amplitude imbalance was compensated considerably so that the estimated position  $\phi$  matched up well with the real position  $\theta$  in experiment.

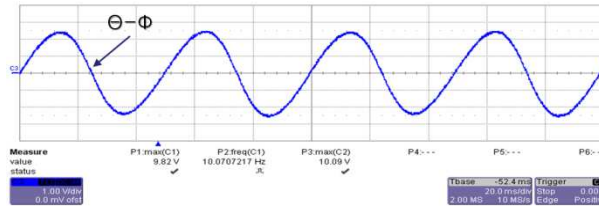
Figs. 11(d) shows waveform of  $Q_r$  and  $D_r$ , Fig. 11(e) shows the first term of  $Q_r$  that is  $A \sin(\theta - \phi)$  and second



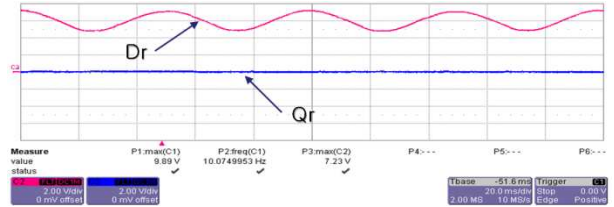
(a)  $\sin$  &  $\cos$  signal



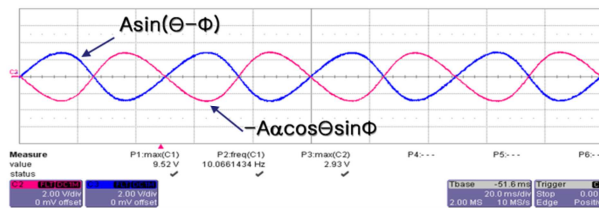
(b) Real position & estimated position



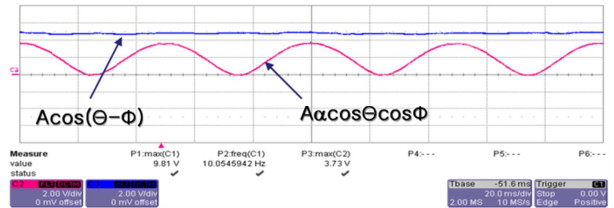
(c) Position error



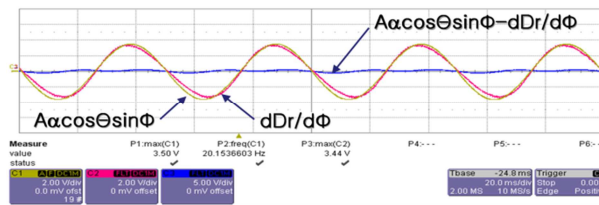
(d)  $D_r$  &  $Q_r$



(e) First and second terms of  $Q_r$



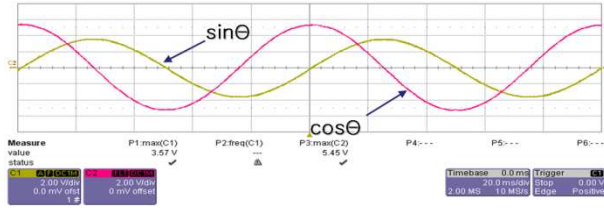
(f) First and second terms of  $D_r$



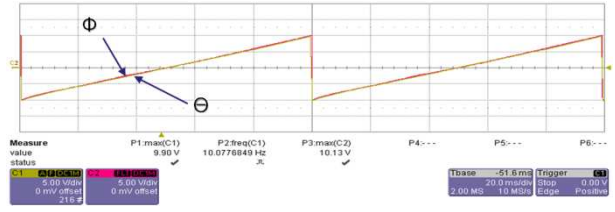
(g)  $\frac{dD_r}{d\phi}$  &  $A \cos \theta \sin \theta$  &  $A \cos \theta \sin \theta - \frac{dD_r}{d\phi}$

Fig. 10. Conventional ATO output signals when unbalanced resolver's output (Experiment)

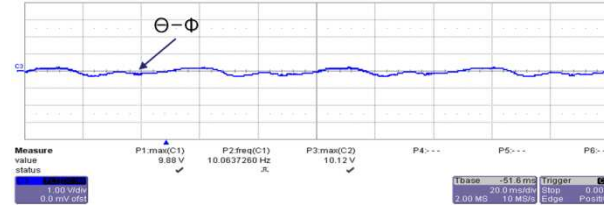




(a) sin &amp; cos signal



(b) Real position &amp; estimated position



(c) Position error

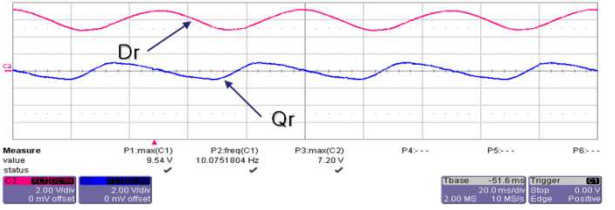
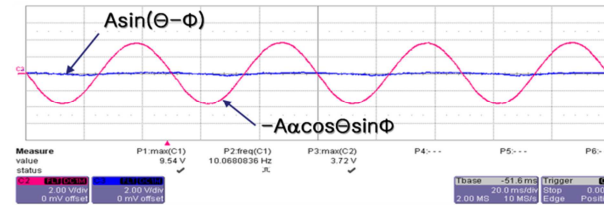
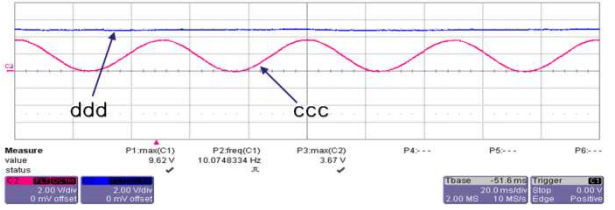
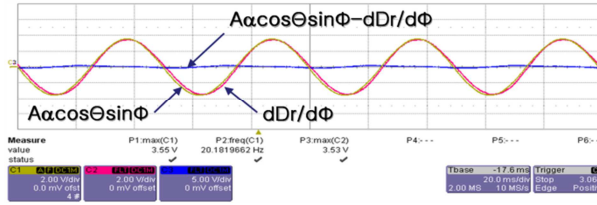

(d)  $D_r$  &  $Q_r$ 

(e) First and second terms of  $Q_r$ 

(f) First and second terms of  $D_r$ 

(g)  $C_{un}$ ,  $A \cos\theta \sin\theta$  &  $C_{un} - A \cos\theta \sin\theta$ 

Fig. 11. Proposed ATO output signals when unbalanced resolver's output (experiment)

term  $-A \cos\theta \sin\phi$ . Fig. 11(f) shows the first term of  $D_r$  that is  $A \cos(\theta - \phi)$  and the second term  $A \cos\theta \cos\phi$ . It can be found the experiment has been carried out well by comparing with the simulation results.

Lastly, Fig. 11(g) shows the difference between amplitude imbalance  $-A \cos\theta \sin\theta$  and the  $D_r$ 's differential  $\frac{dD_r}{d\phi}$ . It can be found that the  $\frac{dD_r}{d\phi}$  value, which is calculated with amplitude imbalance compensation, matches well with amplitude imbalance. As amplitude imbalance part causing imperfect position tracking was removed well, we can also verify the perfect position tracking experimentally.

## 5. Conclusion

This paper suggested the simple RDC algorithm in order to compensate position errors caused by the amplitude

unbalance. The ATO was working after eliminating the unbalanced resolver's output based on  $d$ - $q$  transformation. This RDC is easy, convenient and cost-effective software based scheme. To verify feasibility of RDC scheme, simulations and experiments were carried out. Simulation results showed that the proposed scheme was able to estimate the accurate angle compensating error by the amplitude unbalance. Experimental results were also identical to simulation results. It seems that the industrial could implement the proposed software based RDC easily.

## References

- [1] C. Attaianesi, G. Tomasso, "Position Measurement in Industrial Drives by Means of Low-Cost Resolver-to-Digital Converter," IEEE Transaction on Instrumentation and Measurement, Vol. 56, No. 6, pp.2155-2159,

Dec. 2007

- [2] A. Michalski, J. Sienkiewicz, Z. Watral, "Universal Magnetic Circuit for Resolvers with Different Speed Ratios," *IEEE Instrument and Measurement magazine*, Vol. 10, No. 5, pp.58-68, Oct. 2007
- [3] S. H. Hwang, H. J. Kim, J. M. Kim, L. Liu, H. Li, "Compensation of Amplitude Imbalance and Imperfect Quadrature in Resolver Signals for PMSM Drives," *IEEE Transaction on Industry Applications*, Vol. 47, No. 1, pp.134-143, Jan. 2011
- [4] D. A. Khaburi, "Software-Based Resolver-to-Digital Converter for DSP-Based Drives Using an Improved Angle-Tracking Observer," *IEEE Transaction on Instrumentation and Measurement*, Vol. 61, No. 4, pp. 922-929, Apr. 2012
- [5] S. Sarma, V. K. Agrawa, S. Udupa, "Software-Based Resolver-to-Digital Conversion Using a DSP," *IEEE Transaction on Industrial Electronics*, Vol. 55, No. 1, pp.371-379, Jan. 2008
- [6] J. Bergas, C. Ferrater, G. Gross, R. Ramirez, S. Galceran, and J. Rull, "High-Accuracy All-Digital Resolver-to-Digital Conversion," *IEEE Transaction on Industrial Electronics*, Vol. 59, No. 1, pp. 326-333, Jan. 2012
- [7] L. Ben-Brahim, M. Benammar, M. Alhamadi, N. Alhamadi, M. Alhimi, "A New Low Cost Linear Resolver Converter," *IEEE Sensors Journal*, Vol. 8, No. 10, pp. 1620-1627, Oct. 2008
- [8] L. Ben-Brahim, M. Benammar, M. A. Alhamadi, "A Resolver Angle Estimator Based on Its Excitation Signal," *IEEE Transaction on Industrial Electronics*, Vol. 56, No. 2, pp. 574-580, Feb. 2009
- [9] M. Benammar, L. Ben-Brahim, and M. A. Alhamadi, "A high precision resolver-to-DC converter," *IEEE Transaction on Instrumentation and Measurement*, Vol. 54, No. 6, pp. 2289-2296, Dec. 2005
- [10] L. Idkhajine, E. Monmasson, M. W. Naouar, A. Prata, K. Bouallaga, "Fully Integrated FPGA-Based Controller for Synchronous Motor Drive," *IEEE Transaction on Industrial Electronics*, Vol. 56, No. 10, pp. 4006-4017, Oct. 2009
- [11] R. Hoseinnezhad, A. Bab-Hadiashar, P. Harding, "Position sensing in brake-by-wire callipers using resolvers," *IEEE Transaction on Vehicle Technology*, Vol. 55, No. 3, pp. 924-932, May. 2006
- [12] D. C. Hanselman, "Techniques for improving resolver-to-digital conversion accuracy," *IEEE Transaction on Industrial Electronics*, Vol. 38, No. 6, pp. 501-504, Dec. 1991
- [12] C. H. Yim, I. J. Ha, M. S. Ko, "A resolver-to-digital conversion method for fast tracking," *IEEE Transaction on Industrial Electronics*, Vol. 39, No. 5, pp. 369-378, Oct. 1992
- [13] M. Benammar, L. Ben-Brahim, M. A. Alhamadi, "A novel resolver-to-360° linearized converter," *IEEE Sensors Journal*, Vol. 4, No. 1, pp. 96-101, Feb. 2004
- [14] D. C. Hanselman, "Resolver signal requirements for high accuracy resolver-to-digital conversion," *IEEE Transaction on Industrial Electronics*, Vol. 37, No. 6, pp. 556-561, Dec. 1990
- [15] H. S. Mok, S. H. Kim, Y. H. Cho, "Reduction of PMSM torque ripple caused by resolver position error," *IET Journals & Magazines, Electronics Letters*, Vol. 43, No. 11, pp. 556-561, May. 2007
- [16] S. H. Hwang, Y. H. Kwon, J. M. Kim, J. S. Oh, "Compensation of position error due to amplitude imbalance in resolver signals," *Journal of Power Electronics*, Vol. 9, No. 5, pp. 748-756, Sep. 2009



**Youn-Hyun Kim** (S'01-M'04) He received the B.S., M.S., Ph. D. degrees in electrical engineering from Hanyang University in 1987, 1989, and 2002, respectively. He worked for LG Industrial System Co. as a Senior Research Engineer from 1989 to 1999. He is currently a professor in Department of Electrical Engineering, Hanbat National University. His research areas of interest are Motor Drive, Design and Analysis of Machine, and Power Electronics.



**Sol Kim** He received B.S., M.S., Ph. D. degrees in electrical engineering from Hanyang University in 1997, 1999, and 2004, respectively. He is currently a professor in department of electrical engineering, Yuhan College. His research interests are motor design and motor drives.